Turkish Journal of Electrical Engineering & Computer Sciences

http://journals.tubitak.gov.tr/elektrik/

Research Article

Turk J Elec Eng & Comp Sci
(2015) 23: 885 – 899

doi:10.3906/elk-1302-45

An OFDM throughput analysis for cognitive radio application in contiguous or noncontiguous TV white spaces

Cebrail ÇİFLİKLİ[1], Ahmet Turgut TUNCER[2,*], Yusuf ÖZTÜRK[3]
[1]Department of Electrical and Electronic Engineering, Erciyes University, Kayseri, Turkey
[2]Department of Biomedical Equipment Technology, Vocational School of Technical Sciences, Başkent University, Ankara, Turkey
[3]Department of Electrical & Computer Engineering, San Diego State University, San Diego, CA, USA

Received: 07.02.2013 • **Accepted/Published Online:** 11.06.2013 • **Printed:** 30.04.2015

Abstract: Radio frequency spectrum is a finite and scarce resource. Efficient use of the radio frequency spectrum is a fundamental research issue. Since a large portion of the assigned radio frequency spectrum is used only sporadically, the bands currently allocated to TV services can be opportunistically reassigned to support broadband networking services while continuing to provide broadcast TV. The fragmented and unused TV channels named white spaces have a considerable amount of bandwidth potential and long transmission ranges. Bandwidth scalability can be supported by bonding multiple contiguous or noncontiguous consecutive channels using orthogonal frequency division multiplexing (OFDM)-based cognitive radio.

In this paper, an in-depth throughput analysis of OFDM fixed carrier spacing and fixed carrier number approaches has been done for various modulation schemes in TV white spaces. Signal propagation delay is studied under various channel conditions. An analytical model-based estimation of the throughput by taking into account channel bonding is presented.

Key words: TV white space, channel bonding, fixed subcarrier spacing, fixed subcarrier number, 802.11af

1. Introduction

The proliferation of wireless devices worldwide may increase congestion in the radio frequency spectrum. On the other hand, only 13% or less of the licensed spectrum is being used [1], while a large portion of the assigned spectrum is used only sporadically [2]. The unlicensed spectrum bands (ISM bands), which are populated by various legacy narrowband devices (e.g., Zigbee, 802.11a/b/g) and TV bands, are mostly used sporadically. While the ISM bands are crowded with increased demand as a result of wireless penetration, spread of Bluetooth communication, and machine-to-machine communication, TV bands are underutilized at best. As a finite and scarce resource, efficient use of the radio frequency spectrum emerges as a fundamental research issue. The unused portions of the TV bands referred to as TV white spaces (TVWSs) have the potential to offer a substantial amount of bandwidth and longer transmission ranges. The TV bands, which are 6 MHz wide, can be bonded together and reallocated to support a variety of intermittent networking services while continuing to broadcast TV.

Since the available TVWS may be fragmented in nature, it may be challenging to find a number of contiguous TV channels available specifically in urban areas. Similarly, it will rarely be possible to locate the

*Correspondence: ttuncer@baskent.edu.tr

same number of TV channels to be bonded together. The opportunistic use of multiple TV channels based on availability requires a communication solution supporting channel bonding and variable channel bandwidth.

Opportunistic use of TV bands effectively can be possible via dynamic spectrum access or cognitive radio where transmitter parameters such as frequency band, transmission power, and modulation scheme can be adapted to the environment in which the transmitter operates through changes in software [3].

In the United States, the FCC permitted opportunistic use of TVWS by unlicensed devices [4]. One important requirement imposed on opportunistic transient users is that opportunistic devices deployed in TVWS must not interfere with incumbents, including TV broadcasts and wireless microphone transmissions. This technical and regulatory opportunity prompted the IEEE to create two new committees. The IEEE 802.22 and IEEE 802.11af working committees were formed to develop wireless regional area network (WRAN) and wireless LAN standards, respectively, for operating on vacant TV bands [5,6]. The IEEE 802.22 and 802.11af standards address the use of unlicensed access by fixed and portable devices. Fixed devices (e.g., IEEE 802.22 base stations) are used for providing last-mile broadband access in rural areas, while portable devices can be used to provide short-range wireless connectivity for broadband access (e.g., Wi-Fi-like access points). The large amount of spectrum with its superior propagation characteristics makes the TV bands highly desirable for wireless broadband deployment and usage in rural areas [7].

In a traditional static spectrum allocation scenario, when an incumbent transmission takes place, it is assumed to occupy a predefined TV band entirely. A TVWS device may identify unused or empty spectrum (not used by incumbent or other white space devices) and can utilize the available bandwidth for communication. The effective use of available bandwidth may also necessitate bonding fragmented TVWS bands that are not necessarily contiguous to increase the channel width. A TVWS device must effectively deal with the fragmented nature of the TVWS spectrum, with the possibility of each fragment being of different width. Aggregating contiguous [8–11] and noncontiguous [12–14] channels may result in improved throughput. Consequently, a TVWS device must be able to support dynamic channel width adaptation.

Orthogonal frequency division multiplexing (OFDM) emerged during the last decade as a communication technology capable of supporting a variable channel width through adaptation of the number of subcarriers or subcarrier spacing.

The advantages of channel width adaptation are as follows: first, the traffic can be distributed as evenly as possible across the spectrum to achieve channel load balance. Second, the probability of contention and collision can be greatly reduced by an increased number of orthogonal channels, therefore improving throughput as a result of fewer back-offs and reduced interference. Channel width adaptation has been reported to improve the network performance by 30% to 40% [10]. Third, it allows creating new scenarios where the performance of wireless networks, such as those that employ IEEE 802.11, which uses OFDM technology, can be improved [11].

As a mature technology, OFDM is employed in several wireless technologies such as IEEE 802.11a/g/n Wireless Local Area Network (WLAN or Wi-Fi), IEEE 802.16 Wireless Local and Metropolitan Area Network (WiMAX), and Long-Term Evolution (LTE). Other than its ability to handle multipath fading and intersymbol interference, it offers flexibility of adaptive resource allocation (power, constellation size, and bandwidth) on each individual subcarrier.

In most existing wireless standards, the subcarrier duration is kept constant by allowing the number of subcarriers to vary depending on availability of bandwidth. This approach is named fixed subcarrier spacing (FCS), where the subcarrier spacing is fixed, allowing the number of subcarriers to change with bandwidth availability. When subcarrier spacing is fixed, changes in bandwidth will not require a new design for the PHY

and MAC layer, but preamble and pilot subcarrier allocation need to be reconfigured. A second approach is to fix the number of subcarriers (FCN) while the subcarrier width is allowed to vary based on the channel width available. The bandwidth is chosen large enough to tolerate a certain amount of Doppler spread. In [15–17] the impact of varying the subcarrier bandwidth on the system performance in time- and frequency-selective channels was studied, and an approach for adaptive bandwidth for subcarriers for single-user OFDM was proposed [18,19]. This analysis was extended to a multiuser scenario in [20]. A variable subcarrier width solution for a multiuser OFDM down-link scenario was proposed in [21].

The main contribution of this paper is to study OFDM FCN and FCS physical layer approaches as the basis for operation of cognitive radio in the contiguous and noncontiguous TVWS bands. We investigate the performance of FCN- and FCS-type OFDM solutions on scalable channel width in TV bands focusing on the throughput performance of FCN or FCS schemes. In our analysis, contention-based nonpersistent carrier sense multiple access protocol (np-CSMA) is used to operate in TVWSs as a secondary system in an opportunistic manner and the incumbent TV broadcast channel is considered as a contention-free time division multiple access (TDMA)-based network. Applying this analysis to the IEEE 802.11 type of networks running CSMA/CA, collision avoidance is possible by adding an exponential random backoff time with a fixed mean, in addition to np-CSMA [22]. In this study, we derive a throughput analysis of FCN- or FCS-type OFDM approaches for different modulation and coding schemes. Additionally, this study includes effects of signal propagation delay in analysis results. Based on the analytical and simulation results, the relationship between the throughput and the offered traffic ratio is reported.

The paper is organized as follows. Section 2 provides an overview of related throughput analysis for np-CSMA protocols. In Section 3, OFDM signal analysis for FCN and FCS approaches is introduced. In Section 4, a system model is developed and detailed simulation and performance analysis is provided, and, finally, Section 5 concludes the paper.

2. Throughput analysis

We will first review the analytical approaches and assumptions given in [23] in order to evaluate the performance of a secondary opportunistic CSMA network deployed in TVWS bands. The total arrival process from WS devices in a coverage area is modeled as a Poisson process. Offered traffic (G), which is the total number of packets (newly generated and retransmitted packets) at the TVWS device, is normalized by transmission data rate. Thus,the traffic generated by each TVWS device is statistically modeled with probability P in the joint region of two coverage areas. In this way, the system model accounts for the dynamic behavior of coverage area. It is assumed that the time for carrier sensing is negligible. We consider np-CSMA and focus on the performance of TVWS devices in an infrastructure network deployed on a noiseless channel where an infinite call-call source model is assumed. The fundamental throughput equation can be expressed as [23]:

$$S = \frac{E[U]}{E[B] + E[I]}, \tag{1}$$

where $E[U]$ denotes the expected time length in which no collision occurs and packets are successfully transmitted, and ($E[B] + E[I]$) is the expected busy period plus the following idle period, respectively. The expected time length $E[U]$ over which no collision will occur is given by:

$$E[U] = Ge^{-aG}, \tag{2}$$

where G is offered traffic and a is normalized transmission delay. The transmission will be successful only when:

- Exactly only one ready user senses the medium idle prior to a given transmission slot assigned.
- No new ready user senses the medium idle during the $1/a$ slot time, and the access point does not have interference during the $(\ 1/a+1)$ slot.

The timing diagram of a typical np-CSMA channel is given in Figure 1. The system state alternates between periods (I) in which no station has frames to transmit and busy periods (B) in which at least one station transmits a frame. The total transaction time of a data frame include data frame transmission time and transmission delay. In Figure 1, the normalized total transaction time with respect to data frame transmission time is given as 1 and normalized transmission delay is given as a, respectively.

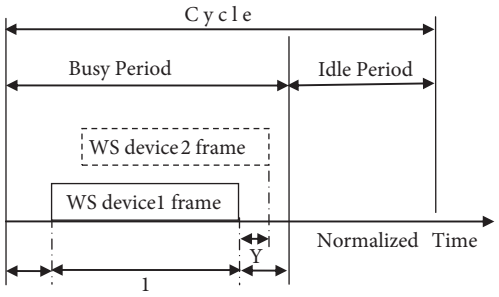

Figure 1. Nonpersistent CSMA timing diagram.

The transmission medium is idle when there is no other packet transmission between the access point and TVWS devices in its coverage region. The expected time length of idle period is defined as $E[I]$ and it is given by:

$$E[I] = \frac{1}{G}. \tag{3}$$

The idle periods are assumed to be independent and geometrically distributed. As shown in Figure 1, the busy period B is the time difference between the first and the last arrivals within a vulnerable period, denoted as Y, plus the data frame transmission time and the signal propagation time. The value of Y is zero if only one transmission occurs in the vulnerable period. The cumulative distribution function of Y can be expressed as:

$$Pr\{Y \leq y\} = e^{-G(a-y)} \quad y \leq a. \tag{4}$$

The expected value of Y can be expressed as :

$$E[Y] = a\frac{\left(1-e^{-aG}\right)}{G}. \tag{5}$$

Using Eq. (5), $E[B]$ can be obtained by:

$$E[B] = E[Y+1+a] = \left(a - \frac{(1-e^{-aG})}{G}\right) + 1 + a. \tag{6}$$

By substituting the expressions for $E[U]$, $E[I]$, and $E[B]$ into Eq. (1), throughput S can be computed as:

$$S = \frac{Ge^{-aG}}{(G(1+a)+e^{-aG})}. \tag{7}$$

3. OFDM signal analysis for FCN and FCS approaches

As the PHY/MAC layer parameters for the White-Fi (IEEE 802.11af) standard have not been finalized yet, we assume its compatibility with the IEEE 802.11a standard to reuse the IP developed. A similar approach has been successfully used in 802.11g development to maximize reuse of IP developed in the 802.11a and 802.11n standards. In this section, we describe the 802.11a PHY and MAC layer briefly and provide analysis of OFDM FCN and FCS cases.

The PHY layer interfaces between the MAC layer and the wireless medium by receiving data frames over the wireless medium and handing it the MAC layer, and vice versa. The PHY layer is responsible for prepending a physical preamble to the data frame, modulating and coding the data packet to the desired data rate. This physical preamble is used to allow the receiver to detect the start of packet transmission and synchronize with the transmitter's data clock. The 802.11a physical layer frame format is shown in Figure 2.

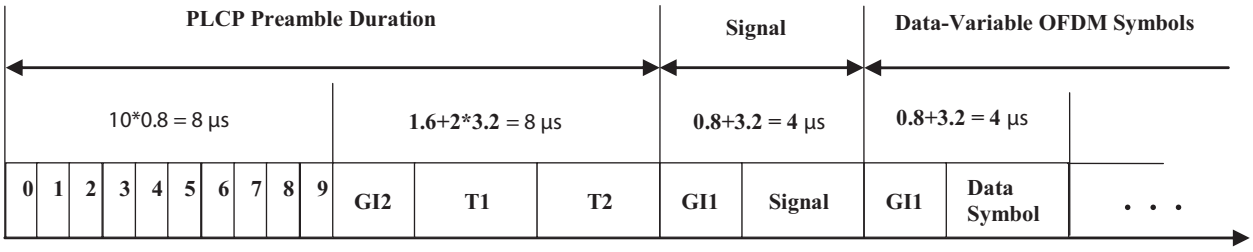

Figure 2. 802.11a physical layer frame format.

The IEEE 802.11a Physical Layer Convergence Protocol (PLCP) preamble begins with 10 short training symbols of 0.8 μs each followed by two long pulses of 4.0 μs each. This preamble sequence allows the receiver to first detect the incoming packet followed by a coarse and fine channel estimation algorithm to estimate channel condition. The first 10 short training symbols are responsible for AGC, diversity selection, coarse frequency offset estimation, and symbol timing. The two long training symbols are used for channel estimation and fine frequency offset estimation. The signal field, always encoded at the lowest data rate, informs the receiver about the encoded data rate and length of the payload. Finally, the payload data are transmitted using an integral number of data symbols modulated and encoded at the scheme specified by the MAC. Each data symbol is 4.0 μs long [24].

IEEE 802.11a specifies data rates ranging from 6 to 54 Mbps. Four different modulation schemes are used: BPSK, 4 QAM, 16 QAM, and 64 QAM. Each higher performing modulation scheme requires a better channel condition for error-free transmission. These modulation schemes are coupled with the various forward error correction convolution encoding scheme to give a multitude of number of data bits per OFDM symbol (N_{DBPS}) performance [24].

The 802.11a PHY specifies a total of 52 OFDM subcarriers with 48 data carrying subcarriers and 4 pilot subcarriers. Each of the subcarriers is spaced 312.5 kHz apart and a guard time of 800 ns is added to each symbol, making the total symbol duration 4 μs [24].

IEEE 802.11 a/g/n networks operate on a fixed 20-MHz channel. Optionally, IEEE 802.11 n nodes can bond two 20-MHz channels into one 40-MHz Wi-Fi channel. On the other hand, TVWS bands are 6 MHz and much narrower than Wi-Fi channels. Following a similar approach to that of IEEE 802.11n, larger channel bandwidth enabling higher throughput can be obtained by combining consecutive TVWS bands when possible.

Multiple contiguous TVWS channels (1, 2, 3, 4, optional 8 and 16) and multiple noncontiguous channels

can be bonded using the OFDM physical layer. Two or more contiguous TVWSs can be merged into a single broad channel to obtain a larger bandwidth by using channel bonding techniques. Noncontiguous TVWSs can be combined by using NC-OFDM, which is capable of deactivating subcarriers across its transmission bandwidth that could potentially interfere with the transmission of other users [12]. The OFDM subcarriers corresponding to the spectrum occupied by local broadcasters, which are determined by sensing measurements, are deactivated or turned "off". This kind of transceiver implementation is called NC-OFDM [12–14]. The data carriers are transmitted on channels not used by the local broadcasters. This is illustrated in Figure 3. In this way, the TV spectrum for Wi-Fi networking is used efficiently. Each 6-MHz TVWS offers a bandwidth of 5 MHz centered at the center frequency of the corresponding TV band. For a single TVWS, the channel width will be 5 MHz. With two channels combined, the total channel width will be 10 MHz, and for four consecutive channels it will be 20 MHz to make use of 802.11a hardware and remain compatible with the 802.11 physical layer.

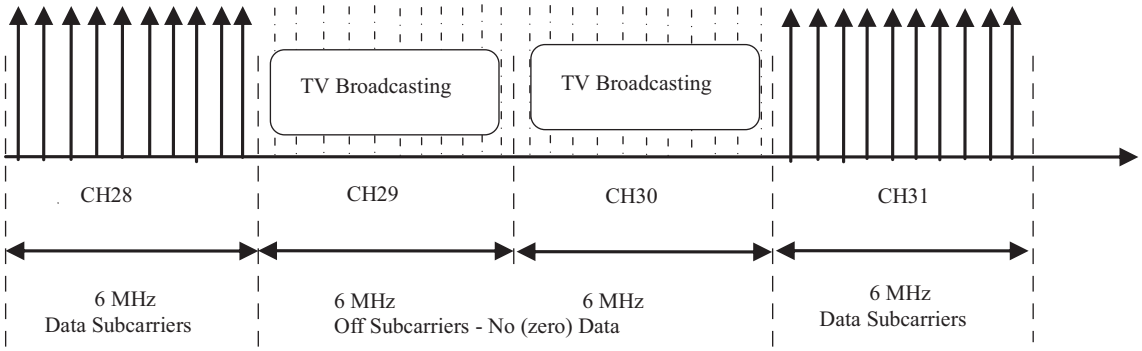

Figure 3. NC-OFDM within 4 consecutive channels.

An 802.11a/g/n OFDM symbol is composed of data, pilot, and null subcarriers. The total number of subcarriers corresponding to fast Fourier transform (FFT) size is N_{FFT}. Let B and ΔF denote channel bandwidth in MHz and subcarrier spacing in KHz, and then $\Delta F = B / N_{FFT}$ and T_{FFT} duration will be $T_{FFT} = 1 / \Delta F$. Consequently, the symbol duration can be written as $T_S = T_{FFT} + T_{GI}$ where $T_{GI} = T_{FFT} / 4$ [24].

In the case of FCN, subcarrier channel size and symbol time will be variable since the numbers of subcarriers are fixed. To be compliant with the IEEE 802.11 protocol family, the number of subcarriers is chosen to be fixed, and then each subchannel will be 78.13 kHz, 156.25 kHz, and 312.5 kHz for operating over 5 MHz, 10 MHz, and 20 MHz on TVWSs, respectively. This in turn causes a change in symbol duration, which would be 12 μs, 6.4 μs, and 3.2 μs for channel widths of 5 MHz, 10 MHz, and 20 MHz, respectively. Forty-eight subcarriers out of 64 subcarriers are used as data subcarriers, 4 subcarriers are used for pilots, and 12 subcarriers are unused as in 802.11 a/g. Several PHY and MAC layer parameters such as symbol duration, PLCP preamble duration, guard interval, etc. will be affected when available bandwidth changes.

In FCS, independent of the bandwidth being used, the subcarrier spacing is fixed. This will in turn result in fixed symbol time with number of subcarriers changing with bandwidth. For the constant subcarrier spacing of 78.13 kHz, the symbol duration (16 μs) and guard interval (3.2 μs) will also be constant for the FCS case. The numbers of subcarriers are chosen are 64, 128, and 256 points for 5 MHz, 10 MHz, and 20 MHz, respectively. Bandwidth changes will not require a new design for the PHY and MAC layer but the preamble and pilot subcarrier allocation need to be reconfigured.

The PHY layer parameters for FCN and FCS for 5, 10, and 20 MHz channel widths are given in Table 1. As observed in the FCN columns of the table, the variables $T_{Preamble}$, T_{Signal}, and T_{Symbol} have their values doubled each time the channel width is divided by two. The reason is that reducing channel width also decreases the width Δf to ensure the orthogonality of the OFDM subcarriers. In the FCS case, all the variables except N_{FFT}, N_{ST}, N_{SD}, and N_{SP} are fixed. Changing the number of data subcarriers (N_{SD}) will affect the modulation dependent variable N_{CBPS} value as shown in Table 2.

The N_{CBPS} variable given in Table 2 represents the number of coded bits of information transmitted in one OFDM symbol. The N_{CBPS} value changes with the number of data subcarriers (N_{SD}) and the channel coding rate R.

Table 1. PHY layer parameters for FCN and FCS for 5, 10, and 29 MHz channel widths.

Parameters	FCN (fixed number of subcarrier)			FCS (fixed channel spacing)		
Bandwidth B (MHz)	5 MHz	10 MHz	20 MHz	5 MHz	10 MHz	20 MHz
FFT size N_{FFT}	64	64	64	64	128	256
No. of data subcarriers N_{SD}	48	48	48	48	110	232
No. of pilot subcarriers N_{SP}	4	4	4	4	6	10
Total no. of subcarriers $N_{ST} = N_{SD} + N_{SP}$	52	52	52	52	116	242
Subcarrier spacing (kHz) $\Delta F = B / N_{FFT}$	78.13	156.25	312.5	78.13		
FFT duration (μs) $T_{FFT} = 1 / \Delta F$	12.8	6.4	3.2	12.8		
PLCP preamble duration (μs) $T_{preamble}$	64	32	16	64		
OFDM symbol duration (μs) $T_{Signal} = T_{FFT} + T_{GI}$	16	8	4	16		
Guard interval (μs) (T_{FFT}/ 4) $T_{GI} = \%\ T_{FFT}$	3.2	1.6	0.8	3.2		
Training symbol GI duration T_{GI2}	1.6	3.2	6.4	6.4		

Table 2. IEEE 802.11 modulation dependent parameters.

Modulation scheme	Coding rate (R)	Coded bits/OFDM symbol N_{CBPS}			
		FCN	FCS		
		5 MHz 10 MHz 20 MHz	5 MHz	10 MHz	20 MHz
BPSK	1/2	48	48	110	232
QPSK	1/2	96	96	220	464
16 QAM	1/2	192	192	440	928
64 QAM	3/4	288	288	660	1393

Changing the channel width will affect the single packet transmission time required. To calculate actual throughput, we need to compute the time required for one single packet's transmission (T_{Packet}). Assuming that the channel is idle when a node senses the channel for transmission, the total transaction time will be determined by DIFS and SIFS, the time required to send the actual data and the time required to send the

acknowledgement:

$$T_{Packet}=T_{BO}+T_{DIFS}+T_{DATA}+T_{SIFS}+T_{ACK}, \tag{8}$$

The single packet transmission time T_{Packet} may be normalized with respect to the packet transmission time T_{DATA} as given in Eq. (9).

$$\frac{T_{packet}}{T_{DATA}}=1+a \tag{9}$$

In Eq. (9), a is the normalized transmission delay equal to $(T_{BO}+T_{DIFS}+T_{SIFS}+T_{ACK})/T_{DATA}$ and is assumed constant since a is normalized relative to the data frame transmission time T_{DATA}. The parameter T_{BO} is the random backoff time for collision avoidance and is assumed as a fixed expectation time in our analysis. The transmission time for the ACK frame (T_{ACK}), distributed IFS (T_{DIFS}), and short IFS (T_{SIFS}) values are all included in the propagation delay constant. T_{DATA} represents the transmission times of a data frame with L bytes of length and its value is expressed as:

$$T_{DATA}=T_{Preamble}+T_{Signal}+T_{Symbol}\times\left\lceil\left(\frac{(16+8*L+6)}{(R*N_{CBPS})}\right)\right\rceil. \tag{10}$$

In Eq. (10), the packet length L, the 16-bit service field for scrambler initiation, and the 6-bit tail are considered when determining the total number of symbols needed to transmit the data frame. The function ceiling $\lceil\bullet\rceil$ is a function that returns the smallest integer value greater than or equal to its argument value. The variables $T_{Preamble}$, T_{Signal}, and T_{Symbol} are the transmission time of the synchronization preamble needed to synchronize with the demodulator, the transmission time of the signal field that indicates to the physical layer the transmission mode, and the symbol duration OFDM physical layer, respectively. When PHY layer parameters for FCN and FCS given in Table 1 are included in the computation of T_{DATA}, we obtain the following.

In FCN,

$$T_{DATA/FCN}=20+4\times\left\lceil\left(\frac{(16+8*L+6)}{(R*N_{CBPS})}\right)\right\rceil. \tag{11}$$

In FCS,

$$T_{DATA/FCS}=20+80+16\times\left\lceil\left(\frac{(16+8*L+6)}{(R*N_{CBPS})}\right)\right\rceil. \tag{12}$$

Eqs. (11) and (12) show the total time required to transmit one packet for fixed carrier number and fixed carrier spacing OFDM variations, respectively. Each data symbol (T_{Symbol}) is 16.0 μs long in FCS. An additional 20-μs signal field on $T_{DATA/FCS}$ is included to guarantee backward compatibility with $T_{DATA/FCN}$ [25].

In addition, all users have the same offered traffic level and generate one packet at a time. It is assumed that the packet transmission time T_{DATA} is constant, as all packets are a constant length for a modulation scheme. The length of a packet is:

$$P_{len}=\frac{T_{DATA}}{T_{Signal}}, \tag{13}$$

the bit rate is:

$$B_{rate}=\frac{8\times L}{T_{DATA}}, \tag{14}$$

and the symbol rate is:

$$S_{rate}=\frac{B_{rate}}{N_{BPSC}}, \tag{15}$$

where N_{BPSC} (the number of data bits in each OFDM subcarrier) is 1 for BPSK, 2 for QPSK, 4 for 16 QAM and 6 for 64 QAM, respectively.

4. Simulation and performance analysis

The system model shown in Figure 4 consists of the two multiple access schemes sharing a single cell or coverage area. Those are the contention-based np-CSMA, used to describe the behavior of a secondary system that has the ability to sense and access a free channel, and TV broadcast channels, which are assumed to form a contention-free TDMA-based network. Each system supplies a number of users that receive information from a single TV tower or base station. The secondary system with all users is assumed to be at a distance from the base station. In this combined system, each user in the CSMA network has access to a database to determine the TV channels that are vacant at that location. It is also assumed that the CSMA client is able to perform clear channel assessment on both CSMA and TDMA channels.

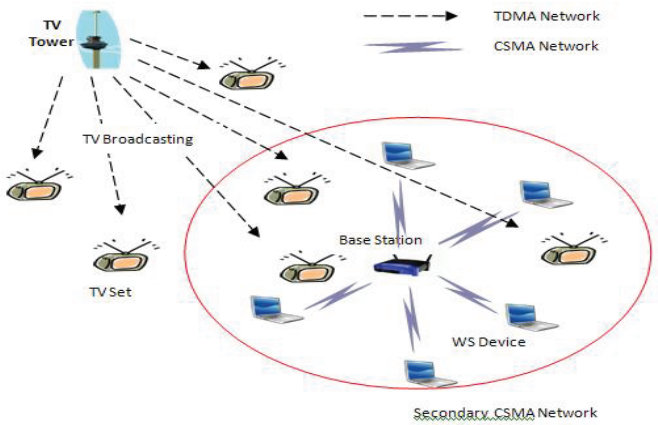

Figure 4. TDMA for primary network and CSMA for secondary network in TV bands.

It is also assumed that the TDMA network uses fixed channel allocation and the TV tower can broadcast television in a predefined TV band.

In order to validate our analytical model, an event-base simulator in MATLAB is devised to simulate FCN/FCS throughput. The throughputs of FCN and FCS schemes are compared by assuming that the IEEE 802.11 distributed coordination function is used for channel management. It is assumed that propagation loss and shadowing are constant. To approximate a Poisson arrival process at the receivers, a sufficient number of trials are generated randomly and independently at each node. The simulation parameters used are given in Table 3.

If the channel is sensed to be busy or a packet goes through a collision, the transmitter schedules the retransmission of the packet after a backoff time, which is equal to the random arrival time in this simulation. In order to compare the throughput of our solution to the np-CSMA model reported in [23], all acknowledgments are assumed to be successful. In addition, all arrival times and retransmissions are assumed to be independent and exponentially distributed. Tables 1 and 2 summarize PHY layer parameters and modulation-dependent

parameters used for FCN and FCS employing 5, 10, and 20 MHz channel widths. The variables used in the simulation related to communication channel, access point, and nodes are given in Table 3. Certain parameters such as the channel bandwidth, frame duration, bit rate, symbol rate, payload length, and modulation and code rate are fixed depending on the objective of each scenario.

Table 3. Simulation conditions.

Variable name	Value
Channel-related	
Normalized propagation delay (a)	0.01
Fixed number of propagation losses	3
Standard deviation of shadowing (dB)	6
Access point-related	
Service area radius (m)	100
Position of the access point (x, y, z) (m)	(0, 0, 5)
Capture ratio (dB)	10
Node-related	
Number of the nodes	100
C/N (dB)	30

In the following discussion, the throughput is calculated for common modulation types considering three scenarios for the FCN and FCS schemes: 1) effect of modulation and coding scheme on throughput, 2) effect of signal propagation delay on throughput, 3) bandwidth efficiencies while varying the modulation scheme for 5, 10, and 20 MHz channel widths, respectively. The payload length is set to 1460 bytes in all experiments.

4.1. Effect of modulation and coding scheme

In this scenario, it is aimed to show the impact of the modulation and coding scheme on the MAC goodput. First, we calculate the normalized transmission time of a single packet for both FCN and FCS and then compute the resulting throughput for different modulation and coding schemes for 5, 10, and 20 MHz channel bandwidth for both analytical and simulated cases. Figure 5 depicts the throughput variation as a function of offered load for FCN and FCS with 5, 10, and 20 MHz channel widths, respectively. Offered load is the total number of packets including newly generated and retransmitted packets at the access point within a time interval and it is normalized by the symbol rate. In Figure 5, offered load is plotted on the x-axis using a logarithmic scale. The normalized propagation delay 'a' was chosen as 0.01 in these experiments.

As can be seen in Figure 5, throughput increases with offered traffic for all modulation options at the beginning of the simulation with increased offered load. It is worth noting that for all the modulation and coding schemes considered in the first scenario, the maximum throughput is reached when offered load is nearly 10. This is the value of offered traffic that results in successful attempts to seize the base station and it remains almost the same. The maximum throughput values obtained in Figure 5 are given in Table 4.

When the 5-MHz channel is considered, both FCN and FCS perform the same since their PHY layer parameters are equal.

A higher fluctuation on MAC throughput can be observed when the frame duration gets shorter, as seen in Figure 5. When the channel bandwidth is 10 MHz, the throughput for the FCS case is a little bit higher than in FCN, depending on the packet size. This may be explained by the fact that the fragmentation capability is disabled in our study. The possibility that a big packet cannot be transmitted is more likely to happen when the frame duration is short, which increases the resulting throughput [26].

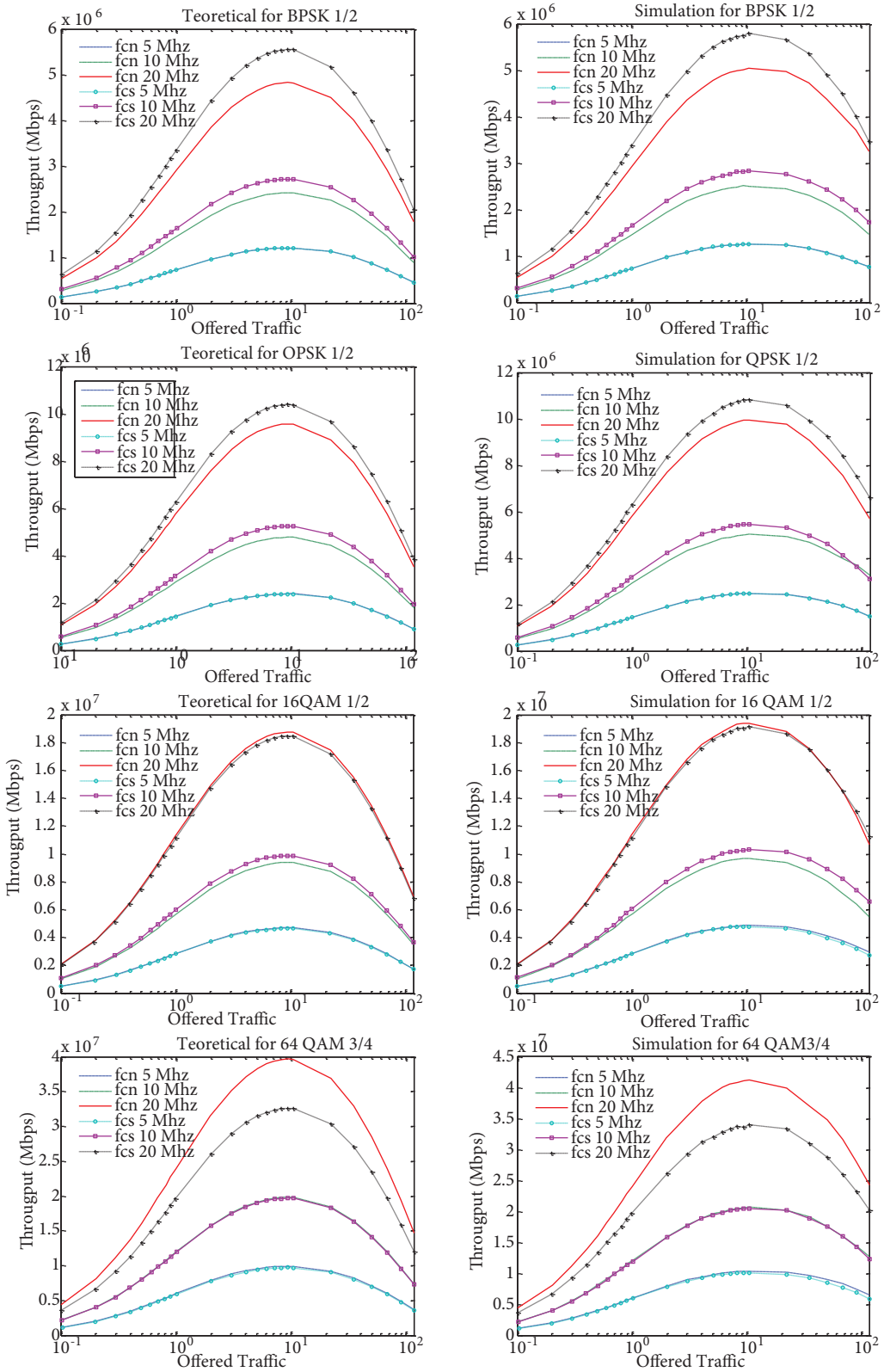

Figure 5. The effect of modulation and coding scheme on FCN and FCS for 1, 2, and 4 contiguous channels.

Table 4. The maximum throughput values from Figure 5.

Modulation scheme		Channel					
		5 MHz		10 MHz		20 MHz	
		Theoretical	Simulation	Theoretical	Simulation	Theoretical	Simulation
FCN	BPSK 1/2	1.21E+06	1.26E+06	2.41E+06	2.52E+06	4.83E+06	5.04E+06
	QPSK 1/2	2.39E+06	2.49E+06	4.78E+06	5.03E+06	9.56E+06	9.96E+06
	16 QAM 1/2	4.69E+06	4.88E+06	9.37E+06	9.67E+06	1.87E+07	1.94E+07
	64 QAM 3/4	9.92E+06	1.04E+07	1.98E+07	2.07E+07	3.97E+07	4.13E+07
FCS	BPSK 1/2	1.21E+06	1.25E+06	2.71E+06	2.83E+06	5.55E+06	5.80E+06
	QPSK 1/2	2.38E+06	2.48E+06	5.26E+06	5.45E+06	1.04E+07	1.08E+07
	16 QAM 1/2	4.64E+06	4.79E+06	9.88E+06	1.03E+07	1.85E+07	1.92E+07
	64 QAM 3/4	9.72E+06	1.01E+07	1.97E+07	2.05E+07	3.26E+07	3.40E+07

On the other hand, with a 20-MHz channel using 64 QAM, FCN slightly outperforms FCS while FCS is better than FCN for BPSK, QPSK, and 16 QAM.

As can be seen in Figure 5, another fluctuation in throughput can be observed between the analytical and simulation results. This is due to the fact that the analytical throughput was obtained under an ideal channel environment where an infinite call source model is assumed and no hidden node exists. In the simulations the capture effect is taken into consideration. As a result, a transmitted packet sometimes survives because of the difference of received power between transmitted nodes.

4.2. Effect of signal propagation delay

In this section, we report the effect of the average transmission delay on MAC throughput. The period between the time at which a packet is generated at a node for transmission to the access point and the time it is received at the access point is the transmission delay. To remove the dependency of transmission delay on the length of the packet, transmission delay is normalized by the packet length in this study. To report the performance of the system for various transmission delays, 16 QAM modulation and rate 1/2 coding scheme are selected on a 20-MHz channel for both FCN and FCS cases. Simulations are performed for normalized propagation delays of 0.01, 0.1, 0.2, and 0.3. The simulation results reporting the throughput for various normalized propagation delay values are shown in Figure 6. The maximum throughput values and their variation for various normalized propagation delay values are given in Table 5.

The simulation results presented in Figure 6 and Table 5 indicate that the throughput is dependent on the normalized propagation delay. A higher fluctuation on MAC throughput can be observed in both the analytical and simulated results for both FCN and FCS cases when the average transmission delay increases. It is interesting that for FCN and FCS, the offered load where the maximum throughput can be achieved is shifted from 10 to 1 when the normalized delay increases to 0.1. This is because increased propagation delay increases the probability of collision and thus degradation in throughput. Table 5 shows that the percent change in maximum throughput and negative signs indicate a reduction in maximum throughput.

4.3. Bandwidth efficiency in modulation schemes

The bandwidth efficiency versus modulation scheme is reported in Figure 7 for both FCN and FCS. It is obvious that a lower modulation constellation means higher efficiency considering the same bandwidth. This is due to the fact that with higher modulation schemes the signaling overhead increases. While throughput of FCS and FCN without signaling overhead increases as the number of subcarrier increases, FCS performs better than

FCN without overhead. If signaling overhead is taken into account the FCS performs better for BPSK, QPSK, and 16 QAM, but FCN is better when the modulation scheme is 64 QAM.

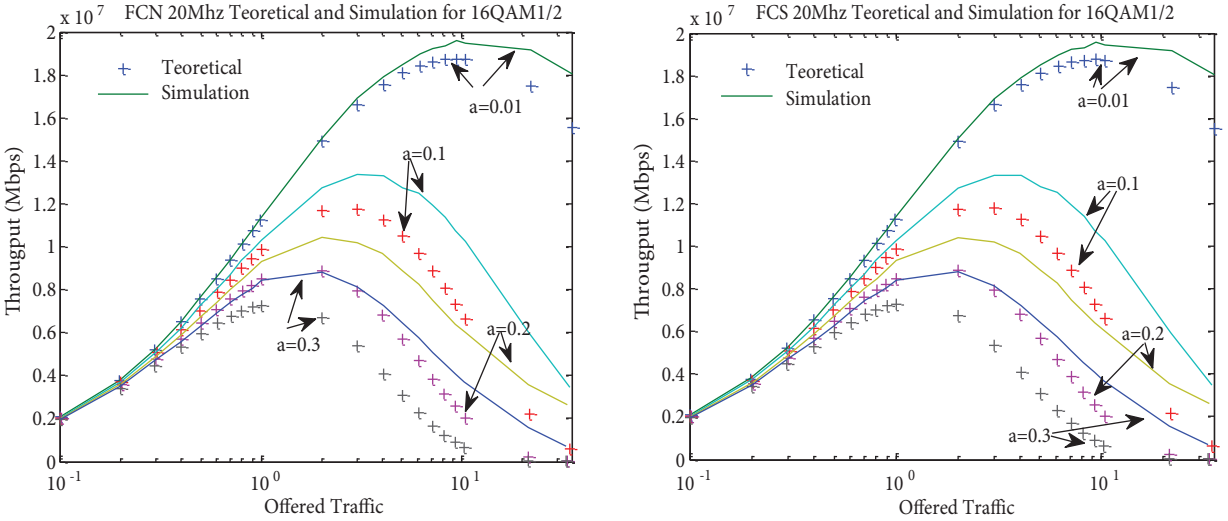

Figure 6. The effect of signal propagation delay on FCN and FCS throughput for 4 contiguous channels.

Table 5. The maximum throughput values from Figure 6.

Normalized propagation Delay 'a'	Theoretical				Simulation			
	FCN	FCS	% in FCN	% in FCN	FCN	FCS	% in FCN	% in FCS
0.01	18.74	18.45			19.58	19.29		
0.1	11.77	11.59	–37.20	–37.22	13.34	12.96	–46.81	–48.83
0.2	8.89	8.75	–24.48	–24.46	10.43	10.33	–27.88	–25.46
0.3	7.28	7.28	–18.06	–16.80	8.79	8.76	–18.70	–17.86

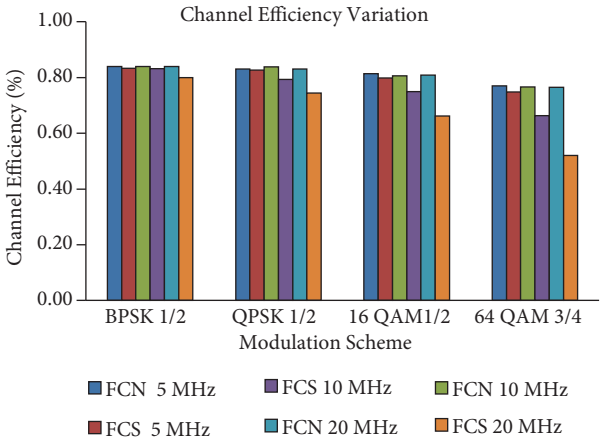

Figure 7. FCN and FCS throughput efficiency versus modulation schemes.

As shown in Figure 7, the FCS and FCN bandwidth efficiencies for 5 MHz are reported as 84% for BPSK, 83% for QPSK, 81% for 16 QAM, and 77% for 64 QAM. On the 10-MHz channel for the FCS case, the bandwidth efficiencies are 83% for BPSK, 79% for QPSK, 75% for 16 QAM, and 52% for 64 QAM. On the

10-MHz channel for FCN, bandwidth efficiencies are 84% for BPSK, 84% for QPSK, 81% for 16 QAM, and 77% for 64 QAM. For the 20-MHz channel, bandwidth efficiencies for the FCS case are 80% for BPSK, 74% for QPSK, 66% for 16 QAM, and 52% for 64 QAM, and for FCN, they are 84% for BPSK, 83% for QPSK, 81% for 16 QAM, and 76% for 64 QAM. Hence, the results indicate that the efficiency of FCN is greater than FCS. For lower modulation schemes the bandwidth efficiency is high for both FCN and FCS cases.

5. Conclusion

In this study, we presented an analysis and simulation framework to investigate the effect of FCN- or FCS-type OFDM technique on changing channel width in contiguous and noncontiguous TV bands.

Three scenarios for the FCN and FCS schemes were considered: 1) effect of modulation and coding scheme on throughput, 2) effect of propagation delay on throughput, 3) and bandwidth efficiencies while varying modulation schemes for 5, 10, and 20 MHz channel widths, respectively.

According to the result obtained for the effect of modulation and coding scheme on throughput, a higher fluctuation in MAC throughput can be observed when the frame duration gets shorter. Indeed, FCN slightly outperformed FCS when the channel bandwidth was 20 MHz using 64 QAM while FCS was better than FCN for BPSK, QPSK, and 16 QAM. When the channel bandwidth was 10 MHz, the throughput for the FCS case was a little bit higher than with FCN, depending on the packet size.

The observations of the effect of signal propagation delay on throughput can be summarized as follows: a higher fluctuation in MAC throughput can be observed in the theoretical and simulation results for both FCN and FCS cases when the average transmission delay gets longer. Finally, the protocol overhead reduced the effective throughput performance drastically. Throughput for FCS and FCN without signaling overhead increased as the number of subcarrier increased. Through simulations we demonstrated that FCN is more efficient than FCS at all times.

It is concluded that additional research should focus on improving the performance of OFDM systems that would be used in TV bands.

References

[1] McHenry MA, McCloskey D, Lane-Roberts G. Spectrum Occupancy Measurements Location 4 of 6: Republican National Convention, New York City, New York August 30, 2004 - September 3, 2004 Revision 2. Vienna, VA, USA: Shared Spectrum Company, 2005.

[2] Federal Communications Commission. Notice of Proposed Rule Making, ET Docket No. 03-22, Oct. 2003. Washington, DC, USA: FCC, 2003.

[3] Mitola J 3rd. Cognitive radio: an integrated agent architecture for software defined radio. PhD, KTH Royal Institute of Technology, Stockholm, Sweden, 2000.

[4] Federal Communications Commission. Unlicensed Operations in the TV Broadcast Bands, Second Memorandum Opinion and Order. ET Docket No. 10-174, Sept. 2010. Washington, DC, USA: FCC, 2010.

[5] Stevenson C, Chouinard G, Lei Z, Hu W, Shellhammer S, Caldwell W. IEEE 802.22: The first cognitive radio wireless regional area networks (WRANs) standard. IEEE Comm Mag 2009; 47: 130–138.

[6] Shin KG, Kim H, Min AW, Kumar A. Cognitive radios for dynamic spectrum access: from concept to reality. IEEE Wirel Commun 2010; 17: 64–74.

[7] Deb S, Srinivasan V, Maheshwari R. Dynamic spectrum access in DTV whitespaces: design rules, architecture and algorithms. In: ACM International Conference on Mobile Computing and Networking; 20–25 September 2009; Beijing, China. pp. 1–12.

[8] Chandra R, Mahajan R, Moscibroda T, Raghavendra R, Bahl P. A case for adapting channel width in wireless networks. In: ACM SIGCOMM Conference on Data Communication; August 2008; Seattle, WA, USA. pp. 135–146.

[9] Moscibroda T, Chandra R, Wu Y, Sengupta S, Bahl P, Yuan Y. Load-aware spectrum distribution in wireless LANs. In: IEEE International Conference on Network Protocols; October 2008; Orlando, FL, USA. pp. 137–146.

[10] Li L, Zhang C. Optimal channel width adaptation, logical topology design, and routing in wireless mesh networks. EURASIP J Wirel Comm 2009; 2009: 940584.

[11] Carvalho CB, Rezende JF. Routing in IEEE 802.11 wireless mesh networks with channel width adaptation. In: IFIP/IEEE MED-HOC-NET 2010**;** June 2010; Juan-les-pins, France. pp. 1–8.

[12] Rajbanshi R, Wyglynski AM, Minden G. An efficient implementation of the NC-OFDM transceivers for cognitive radios. In: Proceedings of CrownCom 2006; June 2006; Mykonos, Greece. pp. 1–5.

[13] Weiss TA, Jondral FK. Spectrum pooling: an innovative strategy for the enhancement of spectrum efficiency. IEEE Comm Mag 2004; 42: 8–14.

[14] Berthold U, Jondral FK, Brandes S, Schnell M. OFDM-based overlay systems: a promising approach for enhancing spectral efficiency. IEEE Comm Mag 2007; 45: 52–58.

[15] Steendam H, Moeneclaey M. Analysis and optimization of the performance of OFDM on frequency-selective time-selective fading channels. IEEE T Comm 1999; 47: 1811–1819.

[16] Harvatin DT, Ziemer RE. Orthogonal frequency division multiplexing performance in delay and Doppler spread channels. In: Proceedings of the IEEE Vehicular Technology Conference; May 1997; Phoenix, AZ, USA. pp. 1644–1647.

[17] Tufvesson F, Maseng T. Multiaccess, Mobility and Teletraffic - Advances in Wireless Networks. Dordrecht, the Netherlands: Kluwer Academic Publishers, 1998.

[18] Das SS, De Carvalho E, Prasad R. Dynamically adaptive bandwidth for sub carriers in OFDM based wireless systems. In: Proceedings of the IEEE Wireless Communications and Networking Conference; 11–15 March 2007; Hong Kong. pp. 1378–1383.

[19] Das SS, De Carvalho E, Prasad R. Performance analysis of OFDM systems with adaptive sub carrier bandwidth. IEEE T Wirel Commun 2008; 7: 1117–1122.

[20] Das SS, De Carvalho E, Prasad R. Variable sub-carrier bandwidth in OFDM framework. Electron Lett 2007; 43:46–47.

[21] Zhang X, Ni Ma. An Adaptive Scheme to Determine the Sub-Carrier Spacing for Multi-Carrier Systems. International Patent No. W0 2010/015102 A1, 11 Feb 2010, 2007.

[22] Huang KC, Chen KC. Interference analysis of nonpersistent CSMA with hidden terminals in multicell wireless data networks. In: Proceedings of IEEE PIMRC '95; 27–29 September 1995; Toronto, Canada. pp. 907–911.

[23] Kleinrock L, Tobagi F. A. Packet switching in radio channels: Part I-Carrier sense multiple-access modes and their throughput-delay characteristics. IEEE T Commun 1975; 23: 1400–1416.

[24] IEEE. Information Technology—Telecommunications And Information Exchange Between Systems-Local and Metropolitan Area Networks—Specific Requirements—Part 11: Wireless LAN Medium Access Control (MAC) and Physical Layer (PHY) Specifications. IEEE Standard 802.11. New York, NY, USA: IEEE, 2007.

[25] Kashyap SN. Channel bonding/loading for TV white spaces in IEEE 802.11af**.** MSc, San Diego State University, San Diego, CA, USA, 2012.

[26] Hiroshi H, Prasad R. Simulation and Software Radio for Mobile Communication. London, UK: Artech House Publisher, 2002.